ResearchGate

See discussions, stats, and author profiles for this publication at: https://www.researchgate.net/publication/230777708

Electronic Structure of Metallouroporphyrins and Their pi-pi Dimers

ARTICLE *in* THE JOURNAL OF PHYSICAL CHEMISTRY · OCTOBER 1984

Impact Factor: 2.78 · DOI: 10.1021/j150665a039

CITATIONS
55

READS
14

1 AUTHOR:

John A Shelnutt
University of Georgia
265 PUBLICATIONS **8,720** CITATIONS

SEE PROFILE

Available from: John A Shelnutt
Retrieved on: 16 January 2016

Electronic Structure of Metallouroporphyrins and Their $\pi-\pi$ Dimers

John A. Shelnutt

Solid State Materials Division, Sandia National Laboratories, Albuquerque, New Mexico 87185
(Received: January 9, 1984; In Final Form: April 13, 1984)

Systematic changes in the UV-visible absorption spectra of metallouroporphyrins are analyzed in terms of the four-orbital model of porphyrin excited states. For metallouroporphyrin monomers a relationship is discovered between the energy separation of the Soret and α bands and the ratio of their transition dipoles squared. The $\pi-\pi$ dimers of these same metallouroporphyrins exhibit a similar, but considerably altered, relationship of this kind. The four-orbital model is shown to predict such relationships and a procedure is given for fitting the spectral data. Values for the molecular orbital parameters of the model result. Further analysis of the changes in these orbital parameters allows determination of the shifts in the highest-filled and lowest-empty π orbitals of the porphyrin ring. It is shown that metal-dependent shifts in the frontier-orbital energies are similar for both monomers and dimers. Dimerization results in distinctive shifts in orbital energies that are independent of the metal incorporated into the porphyrin core. Dimerization also causes a change in the transition dipoles of the $\pi \rightarrow \pi^*$ transitions that give rise to the α and Soret bands.

Introduction

Metallo*uroporphyrins*, unlike other natural metalloporphyrins, aggregate in aqueous alkaline solution only at high concentrations (>0.01 M).[1,2] On the other hand, they can be forced to aggregate at low concentrations by addition of molar amounts of salt or by acidification.[1-6] Typically addition of salt results in aggregates (probably dimers) that remain in solution, whereas larger aggregates which form in acidic solutions tend to flocculate and precipitate.

In spite of these different properties both the salt dimer and the acid aggregate have similar absorption spectra.[1-6] In addition, the changes in the UV-visible absorption spectra observed upon aggregation are similar regardless of the metal contained in the uroporphyrin core. The spectral changes are most pronounced for the Soret band, which shows a severe broadening and a blue shift of 10-15 nm. The α and β bands are also broadened, but undergo a smaller red shift.

Surprisingly, in spite of these relatively large changes in the $\pi \rightarrow \pi^*$ transitions, one observes almost no change in the vibrational spectrum of the porphyrin moiety. For example, the Raman spectrum in the marker-line region between 1300 and 1700 cm^{-1} shows only small shifts of about 2-3 cm^{-1}.[3-6]

In order to gain a deeper understanding of these remarkable spectral changes and the associated electronic structure differences between the π electron systems of the porphyrin in the monomer and dimer, a series of metallouroporphyrin derivatives were examined with absorption and resonance Raman difference spectroscopy. The companion report[3] describes these results and developes a model of the aggregation process. The goal of this report is to analyze the systematic differences in the spectra of the metallouroporphyrin monomers and dimers. Gouterman's four-orbital model of porphyrin excited states[7] has been sucessfully applied to the problem. The four-orbital model quantitively predicts various trends in the experimental data and the values of a number of important molecular orbital parameters are given by the analysis. The analysis provides a clearer picture of the metal-porphyrin interaction and the porphyrin-porphyrin interaction in the $\pi-\pi$ dimer.

In the theoretical treatment of the dimer problem given here exciton coupling (V in ref 8) is ignored and only the "solvent" interaction resulting from dimerization (D in ref 8) is considered.[8,9] Nevertheless, it can be shown that the solvent interaction (neglected in previous work[8,9]) can account for the spectroscopic changes, in particular the blue shift in the Soret band. However, because of the large experimental uncertainties for the dimer results, a sizable exciton coupling cannot be ruled out and, in fact, is predicted. Both the solvent and exciton coupling can be treated in a more elaborate extension of the methods given in the present work.[10] For example, expressions 6 and 9 below can be generalized to include both interactions V and D explicitly. Preliminary results using a dipole-dipole exciton-coupling analysis to fit the experimental data indicate that a strong solvent effect is required for an adequate fit. Current efforts to quantitatively determine the relative contributions of the exciton and solvent interactions to the spectral changes are focused on obtaining more accurate spectral data using curve-fitting routines to analyze the broad dimer spectra and investigations of other metalloporphyrin dimer systems.[10]

Results

Table I lists spectral parameters for a number of metallouroporphyrins and dimers. The absorption spectra of these nonhyper[11] metalloporphyrins are typical, containing only the strong Soret or B band near 400 nm and a weaker pair of bands in the visible, called α and β, which are the 0-0 and 0-1 components of the Q transition. The wavelengths of the α band (λ_Q) and Soret band (λ_B) are given in Table I along with the ratios of their oscillator strengths, f_Q/f_B. The energy separation, $E_B - E_Q$, between the Soret- and α-band maxima is also tabulated for both monomers and dimers.

The oscillator strengths, f_Q and f_B, are the integrated intensities of the absorption bands. The values given in Table I are averages obtained from several methods of integrating the intensities (e.g., $f \sim A\Delta\nu$, where A is the absorbance at the peak and $\Delta\nu$ is the width at half-maximum).[12] The possible errors are about ±10% for the monomers and are even larger (±20%) for the dimers because of the broadness of the bands. Most of the error comes from attempts to separate background from the tail of the Soret band in the Q-band region and from decomposing the overlapping α and β bands. Errors in $E_B - E_Q$ are ±100 cm^{-1} for the monomers, and, again, are somewhat larger (±200 cm^{-1}) for the dimers due to broadening.

(1) Blumberg, W. E.; Peisach, J. *J. Biol. Chem.* **1965**, *240*, 860-876.
(2) Mauzerall, D. *Biochemistry* **1965**, *4*, 1801-1810.
(3) Shelnutt, J. A.; Dobry, M. M.; Satterlee, J. D. *J. Phys. Chem.*, preceding article in this issue.
(4) Shelnutt, J. A. *J. Phys. Chem.* **1983**, *87*, 605-616.
(5) Shelnutt, J. A. *Inorg. Chem.* **1983**, *22*, 2535-2544.
(6) Shelnutt, J. A. *J. Am. Chem. Soc.* **1981**, *103*, 4275-4277.
(7) Gouterman, M. *J. Chem. Phys.* **1959**, *30*, 1139-1161.
(8) Gouterman, M.; Holten, D.; Lieberman, E. *Chem. Phys.* **1977**, *25*, 139-153.
(9) Selensky, R.; Holten, D.; Windsor, M. W.; Paine, J. B.; Dolphin, D.; Gouterman, M.; Thomas, J. C. *Chem. Phys.* **1981**, *60*, 33-46.
(10) Shelnutt, J. A., *manuscript in preparation.*
(11) Gouterman, M. In "The Porphyrins"; Dolphin, D., Ed.; Academic: New York, 1978; Vol. 3, pp 1-165.
(12) Mulliken, R. S. *J. Chem. Phys.* **1939**, *7*, 14-20.

0022-3654/84/2088-4988$01.50/0 © 1984 American Chemical Society

TABLE I: Spectral Parameters for Metallouroporphyrin Monomers and Dimers[a]

metal	λ_Q, nm	λ_B, nm	f_Q/f_B	$E_B - E_Q$, cm^{-1}	θ, deg	$2A_{1g}$, cm^{-1}		$^1/_2(E_B + E_Q)$, cm^{-1}
Pt	533	378	0.0795	7693	8.8	2300	M[b]	22608
	537	367	0.0509	8626	16.4	4670	D[b]	22935
Ni	551	390	0.0626	7476	6.8	1750	M	21895
	554	377	0.0440	8475	15.6	4390	D	22288
Cu	562	398	0.0488	7333	4.9	1250	M	21460
	565	382	0.0309	8479	14.2	3920	D	21939
Zn	572	406	0.0308	7148	2.0	510	M	21057
	581	396	0.0188	8048	11.5	3080	D	21232
Pd	544	389	0.0614	7276	6.3	1620	M	22045
	549	380	0.0433	8166	14.8	4120	D	22265
VO(MV^{2+})	574	402	0.0427	7454	4.2	1070	M	21149
	578	397	0.0312	7888	12.7	3440	D	21245
Mg(Pyr)	581	408	0.0177	7298	≈0	0	M	20876
$Sn(OH)_2$	574	404	0.0214	7331	≈0	0	M	21087

[a] The data are taken mostly from ref 3. [b] M denotes monomer, D dimer.

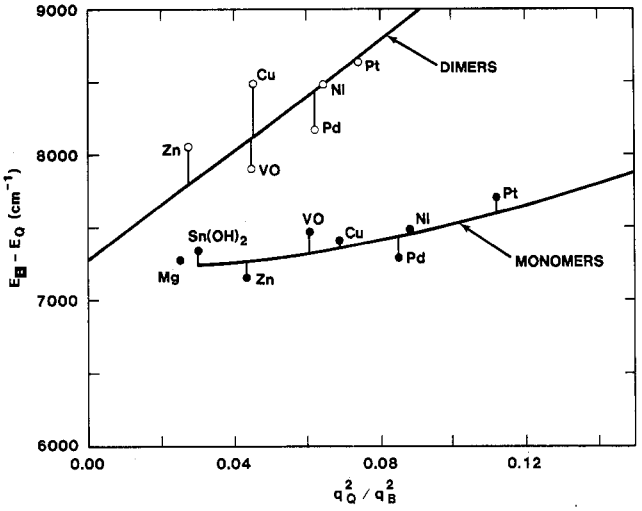

Figure 1. Plot of energy separation of the Soret and α bands vs. the ratio of their transition dipoles for metallouroporphyrin monomers (●) and dimers (○). The curves through the data points are theoretical (see text).

The systematic variation in these spectral parameters is best displayed by plotting the separation between the Soret and α band vs. the ratio of the dipole strengths of the α and Soret bands, q_Q^2/q_B^2, as shown in Figure 1. (The transition dipole q is related to the oscillator strength f by the relation, $f \sim Eq^2$.) The reason for plotting the data in this way will be clear later. It is obvious from Figure 1 that the nature of the metal systematically perturbs the absorption spectrum and, in addition, that the relationship between the two spectral parameters is different for the monomers and dimers. The scatter in the data is not much worse than the experimental uncertainties.

Discussion

Four-Orbital Model of Porphyrin Excited States.[7,11] The theoretical curves through the data points plotted in Figure 1 are obtained from an analysis based on Gouterman's four-orbital model of metalloporphyrin excited states. The four-orbital model describes the systematic variation in the absorption spectra of porphyrins containing distinct metals in terms of a perturbation on idealized porphyrin electronic states obtained from excited-state molecular orbital configurations. The curves in Figure 1 result from the relationship between band energies and intensities that is predicted by the model. Following Gouterman[7] we will now derive a relationship between $E_B - E_Q$ and q_Q^2/q_B^2 in terms of three of the four molecular orbital parameters defined below. In following this procedure we are tacitly assuming that the variation in the spectra results from systematic differences in these three parameters. We are also presupposing that the totally symmetric component of the metal–porphyrin and the porphyrin–porphyrin interactions dominate.

In the four-orbital model the Q and B electronic states result from $\pi \rightarrow \pi^*$ transitions from the two highest filled molecular orbitals, $a_{1u}(\pi)$ and $a_{2u}(\pi)$, to the first unfilled orbital, $e_g(\pi^*)$. The two excited-state configurations ($a_{1u}^1 a_{2u}^2 e_g^1$ and $a_{1u}^2 a_{2u}^1 e_g^1$) are nearly degenerate as a result of the near degeneracy of the a_{1u} and a_{2u} orbitals. Because these excited-state configurations have the same symmetry, they can and do strongly interact via the two-electron term of the molecular Hamiltonian. Gouterman defines the matrix element coupling the excited-state configurations as A_{1g}''. A_{1g}'' acts to mix the configurations, which have energies $E(a_{1u}^1 a_{2u}^2 e_g^1) = A_{1g}' - A_{1g}$ and $E(a_{1u}^2 a_{2u}^1 e_g^1) = A_{1g}' + A_{1g}$, to give the observed excited states Q and B, with energies E_Q and E_B. These expressions for the configuration energies introduce the molecular orbital parameters A_{1g}' and A_{1g}. A_{1g}' is defined as the average energy of the two excited-state configurations.

$$A_{1g}' = \tfrac{1}{2}[E(a_{1u}^1 a_{2u}^2 e_g^1) + E(a_{1u}^2 a_{2u}^1 e_g^1)] = \tfrac{1}{2}[2E(e_g) - E(a_{1u}) - E(a_{2u})] \quad (1)$$

A_{1g} is defined as half the difference in the transition energies of the excited-state configurations.

$$A_{1g} = \tfrac{1}{2}[E(a_{1u}^2 a_{2u}^1 e_g^1) - E(a_{1u}^1 a_{2u}^2 e_g^1)] = \tfrac{1}{2}[E(a_{1u}) - E(a_{2u})] \quad (2)$$

A_{1g} is also just one-half the energy difference between the a_{1u} and a_{2u} orbitals.

The matrix element A_{1g}'' strongly mixes the configurations so that a better basis set is made up of the states B^0 and Q^0, defined as the symmetric and antisymmetric combinations of the configurations, respectively. The energies of the new states are $E_{Q^0} = A_{1g}' - A_{1g}''$ and $E_{B^0} = A_{1g}' + A_{1g}''$. These states are near the correct energy eigenstates, because they are coupled only by the matrix element A_{1g}'', which is small due to the near degeneracy of the a_{1u} and a_{2u} orbitals.

The states Q and B can be found by exact diagonalization of the Hamiltonian by introducing the parameter θ which "unmixes" the 50/50 mixed states Q^0 and B^0. These new states are linear combinations of Q^0 and B^0 given by Gouterman[7]

$$Q_y \equiv -\sin\theta\, B_y^0 + \cos\theta\, Q_y^0$$
$$B_y \equiv \cos\theta\, B_y^0 + \sin\theta\, Q_y^0 \quad (3)$$

with similar expressions for the x components.[13] The unmixing parameter θ is defined in terms of the MO parameters by

$$\tan 2\theta = A_{1g}/A_{1g}'' \quad (4)$$

Transitions to the Q and B states give the α and Soret absorption

(13) Shelnutt, J. A. *J. Chem. Phys.* **1981**, *74*, 6644–6657.

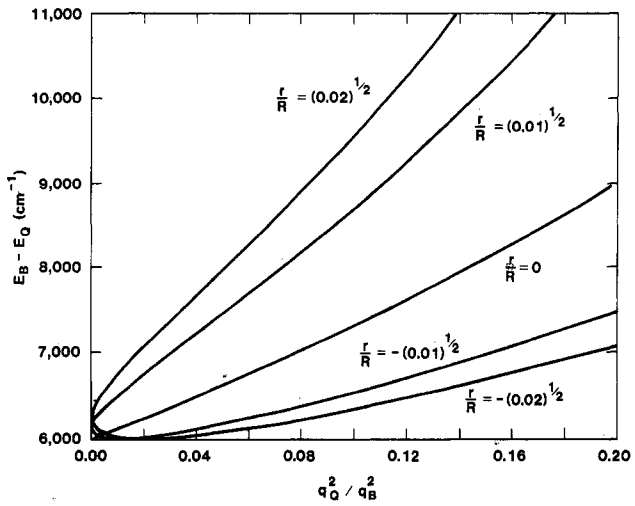

Figure 2. A family of theoretical curves of $E_B - E_Q$ vs. q_Q^2/q_B^2 generated by varying A_{1g} for discrete values of r/R and holding A_{1g}'' constant.

bands, respectively. The β band is a vibrational side band of the Q(0–0) transition.

The energies of these states in terms of the molecular orbital parameters A_{1g}, A_{1g}', and A_{1g}'' are

$$E_Q = A_{1g}' - A_{1g}''/\cos 2\theta$$
$$E_B = A_{1g}' + A_{1g}''/\cos 2\theta \quad (5)$$

We now see that $E_B - E_Q$, which is the ordinate in Figure 1, is given by

$$E_B - E_Q = 2A_{1g}''/\cos 2\theta \quad (6)$$

and only involves two of the MO parameters A_{1g}'' and A_{1g} via θ.

Along the abcissa in Figure 1 the ratio of the squares of the transition dipoles for Q and B is plotted. The transition dipoles squared can also be expressed in terms of MO parameters given by Gouterman[7]

$$q_Q^2 = R^2 \sin^2\theta - rR \sin 2\theta + r^2 \cos^2\theta$$
$$q_B^2 = R^2 \cos^2\theta + rR \sin 2\theta + r^2 \sin^2\theta \quad (7)$$

where r and R are the transition dipoles of the 50/50 mixed configurations Q^0 and B^0, respectively. They can be defined further in terms of the transition dipoles for the configurations. If R_1 is the dipole matrix element for the transition $a_{1u} \rightarrow e_g$ and R_2 is the dipole matrix element for $a_{2u} \rightarrow e_g$, then R and r are the sum and difference of R_1 and R_2, i.e.

$$R = (2)^{-1/2}(R_1 + R_2)$$
$$r = (2)^{-1/2}(R_2 - R_1) \quad (8)$$

We now have the expression for q_Q^2/q_B^2 in terms of the three MO parameters r/R, A_{1g}, and A_{1g}''.

$$q_Q^2/q_B^2 = \frac{\sin^2\theta - \frac{r}{R}\sin 2\theta + \left(\frac{r}{R}\right)^2 \cos^2\theta}{\cos^2\theta + \frac{r}{R}\sin 2\theta + \left(\frac{r}{R}\right)^2 \sin^2\theta} \quad (9)$$

The fourth MO parameter A_{1g}' is not involved in the relationship between $E_B - E_Q$ and q_Q^2/q_B^2.

If suitably accurate molecular orbital calculations existed for all of the molecules represented in Figure 1, we could use the calculated parameters A_{1g} and r/R given A_{1g}'' to predict the relationship between $E_B - E_Q$ and q_Q^2/q_B^2. In lieu of calculations we can vary the parameters to obtain a fit to the experimental data, thereby determining the values of the MO parameters. Since only a limited family of curves can be generated by varying the parameters, the ability to fit the data in Figure 1 also acts as a stringent test of the four-orbital model.

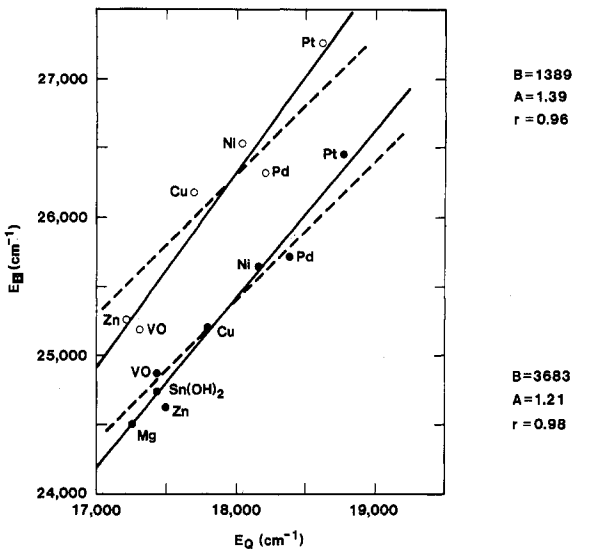

Figure 3. Plot of E_B against E_Q for metallouroporphyrin monomers (●) and dimers (○). Solid lines are linear least-squares fits, and dashed lines show a slope of 1.

Figure 2 shows a family of curves generated for discrete values of r/R by continuously varying A_{1g} (i.e., θ) while holding A_{1g}'' constant. It is immediately apparent that this family of curves shows the general behavior of the relationships between $E_B - E_Q$ and q_Q^2/q_B^2 exhibited by the experimental data (Figure 1). Explicitly, the required features are (1) nearly linear dependence in the region beyond $q_Q^2/q_B^2 = (r/R)^2$, (2) nearly equivalent $E_B - E_Q$ axis intercepts for the extrapolated linear portions of both curves, and (3) strong dependence of the slopes of the linear part of the curves on r/R so that it may be possible to fit both monomer and dimer data by varying r/R.

Specifically, the curves generated all have a minimum at $E_B - E_Q = 2A_{1g}''$ (arbitrarily chosen to be 6000 cm^{-1} for calculations displayed in Figure 2), and the value of q_Q^2/q_B^2 at the minimum is just $(r/R)^2$. Equation 9 simplifies for $r/R = 0$ to $q_Q^2/q_B^2 = \tan^2\theta$. Because $1/\cos 2\theta \approx 1 + 2\tan^2\theta$ for $\theta < 1$, the curve for $r/R = 0$ is nearly linear with slope near $4A_{1g}''$ and intercept $2A_{1g}''$. Negative values of r/R give curves with slopes less than $4A_{1g}''$; positive values give slopes larger than $4A_{1g}''$ (see Figure 2).

Application to Metal-Dependent and Aggregation-Dependent Spectral Changes. The data presented in Figure 1 clearly indicate very different slopes for monomer and dimer curves, but nearly equal intercepts. A least-squares linear fit through the monomer data points gives a slope of about 4000 cm^{-1} and intercept near 7100 cm^{-1}. Thus, $2A_{1g}''$ is necessarily in the neighborhood of 7100 cm^{-1}, and the slope is clearly less than $4A_{1g}''$. Therefore, a negative value of r/R is required for the monomer fit. The fit shown in Figure 1 is generated with $2A_{1g}'' = 7250$ cm^{-1} and $r/R = -0.173$ [$(r/R)^2 = 0.03$].

Using the same value of $2A_{1g}''$ we can fit the dimer data as well but with $r/R = 0.022$ [$(r/R)^2 = 0.0005$]. The small value for r/R is expected because the slope of the linear fit is close to $4A_{1g}''$ for the dimer data.

The ability of the four-orbital model to predict the correct functional relationship between the two spectroscopic parameters confirms the model's quantitative validity. More importantly we can now use the values generated by fitting the experimental data to gain a detailed understanding of the effects of varying the metal on the electronic structure of the π-electron system of the ring. Similarly, the effects of the porphyrin–porphyrin interaction in the π–π dimer can now be elucidated. However, before we turn to this task we compare the value we have obtained for A_{1g}'' for the uroporphyrins with earlier estimates of A_{1g}'' for other porphyrins.

Comparison with Earlier Work. The value of 7250 cm^{-1} for $2A_{1g}''$ compares favorably with earlier estimates of A_{1g}''. In Gouterman's early work he obtained an estimate of 6700 cm^{-1}

for $2A_{1g}''$ for metallotetraphenylporphyrins by neglecting any θ dependence so that expression 6 becomes $E_B - E_Q = 2A_{1g}'' =$ constant. Then Gouterman showed that a plot of E_B vs. E_Q is linear with a slope near unity and intercept of 6700 cm^{-1} (assuming slope 1) for the series of metallotetraphenylporphyrins.[7]

Figure 3 shows the corresponding plot of E_B vs. E_Q for the metallouroporphyrins. The lower dashed line has slope 1 and intercepts the E_B axis at 7400 cm^{-1}. Thus, $2A_{1g}''$ would be estimated to be 7400 cm^{-1} for the metallouroporphyrins if we ignore the θ dependence of $E_B - E_Q$ as Gouterman did. However, the solid line is a least-squares fit to the data showing that the slope is actually 1.2 and the intercept is 3700 cm^{-1}. Note that the least-squares line for the dimer data has an even greater slope of 1.4. The fact that θ varies for the metals in this series explains why slopes different from 1 can be observed in a plot of E_B vs. E_Q.

We conclude that the value of 7250 cm^{-1} for $2A_{1g}''$ from a fit using the θ-dependent expressions is in good agreement with the value of 7400 cm^{-1} for the uroporphyrins obtained by using Gouterman's approximate method and it is also in fair agreement with the value of 6700 cm^{-1} obtained by Gouterman for the tetraphenylporphyrins.

Metal Effects on a_{1u} and a_{2u} Orbitals. After the values of A_{1g}'' and r/R are set, varying A_{1g} generates the curves in Figures 1 and 2. Therefore, it is the value of A_{1g} for each metal that determines its position along the curve. The value of θ, from which A_{1g} can be calculated by using eq 4, has been determined at each point along the theoretical curves in Figure 1 and can be estimated for each metal. The value of θ for each metal is given in Table I along with the value of $2A_{1g}$ calculated from θ. The monomers have low values of θ ranging from 0–8.8°, whereas the values for the dimers range between 11.5 and 16.4°. The value of θ for monomer and dimer differ by 7.6–9.5°. From eq 1, $2A_{1g}$ is just the separation between the a_{1u} and a_{2u} orbital energies. The splitting of the a_{1u} and a_{2u} orbitals thus ranges from near 0 cm^{-1} for Mg and $Sn(OH)_2$ to 2300 cm^{-1} for Pt for monomeric uroporphyrins and from 3080 cm^{-1} for Zn to 4670 cm^{-1} for Pt for the dimers. These are significant changes in the orbital energies, since changing metals can result in up to a difference of 0.3 eV in the separation of the top filled π orbitals.

It is interesting to consider how changes in the metal–porphyrin interaction can bring about such changes in the frontier orbitals. Since the $a_{1u}(\pi)$ orbital has nodes at the nitrogens, the metal perturbation is sensed mainly by the a_{2u} orbital, which in contrast places considerable charge density on the pyrrole nitrogens. It is apparent (from the metal-dependent changes in $2A_{1g}$) that the series of metals from Mg to Pt interact with a_{2u} decreasing its energy by as much as 2300 cm^{-1}, with the more electronegative metals having the lower a_{2u} energy. The approximate energy levels for the different metals are illustrated schematically in Figure 4. The stabilization of the a_{2u} orbital probably results from increasing interaction with an empty p_z orbital of the metal.[7,14,15]

The pattern of shifts in the Raman marker lines is also consistent with the suggestion that the metal–porphyrin interaction primarily affects the a_{2u} orbital. The a_{2u} orbital places charge density mainly on the meso-carbons and pyrrole nitrogens. The motion of the meso-carbons is known to be the largest contributor to the core-size marker lines.[16] Changing the metal for the series of metals represented in Figures 1 and 4 results in large shifts in the Raman core-size marker lines, but only small shifts in the oxidation-state marker line ν_4.[5,14,15]

Effect of Dimerization on the a_{1u} and a_{2u} Orbitals. Dimerization results in a shift of about 2500 cm^{-1} in the a_{1u} orbital with respect to the a_{2u} orbital. The dimer shift only weakly depends on the metal in the ring. The dimer shift may result from an increase in the a_{1u} orbital, a decrease in the a_{2u} orbital, or both. Without further information we cannot distinguish among these three possibilities. The Raman marker line shifts may provide the needed information. Because the pattern of Raman line shifts observed upon changing the metal[14] and upon dimerization are distinct, we may speculate about the three possibilities.

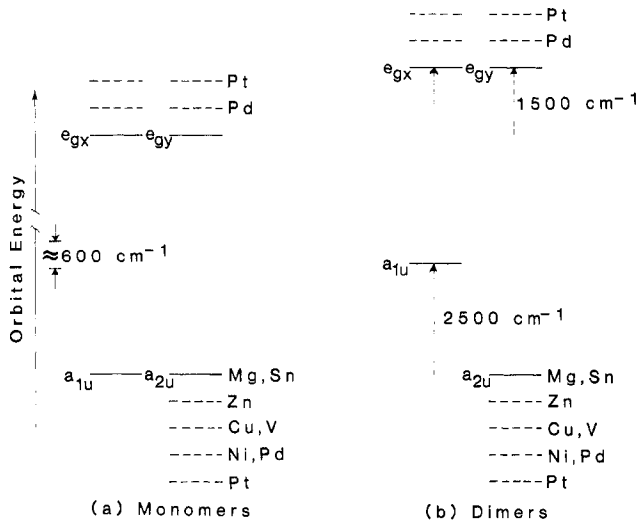

Figure 4. Energy level schemes for monomers (a) and dimers (b) obtained by using the values of the molecular orbital parameters found by fitting the experimental data.

Upon dimerization only small, approximately equal increases (2–3 cm^{-1}) in the core-size marker lines and ν_4 are observed.[3-5] Because the marker line shifts associated with stabilization of the a_{2u} orbital involve large shifts in the core-size lines relative to the shift in ν_4 and because this pattern of Raman shifts is not observed upon dimerization, we conclude that the a_{2u} level does not change. The a_{1u} orbital energy must, therefore, increase upon dimerization. It is also true that a relatively large increase in the a_{1u} level is only weakly reflected in the Raman marker lines giving small, and nearly equal, shifts to higher frequency in the spectra of the dimer relative to the monomer.

It is not clear what the interaction between porphyrin rings in the dimer entails. However, if the above analysis is correct and it is the a_{1u} orbital that is primarily affected, then the orbital densities may shed some light on the mechanism of interaction.[7] On the basis of the dissimilarity in distribution of charge for the two orbitals it is reasonable to expect a quite different response of the Raman marker vibrations to changes in the a_{1u} and a_{2u} orbital energies as is observed. The a_{1u} orbital places charge on the α and β carbons of the pyrrole rings, while the a_{2u} places little charge at these positions. Furthermore, a_{1u} has nodes through the pyrrole nitrogens and the meso-carbons where the a_{2u} orbital places charge density. Thus, dimerization apparently involves interactions between the α- and β-carbon positions in the porphyrin rings of the dimer as opposed to the nitrogen and meso-carbon positions. The core-size marker lines all contain secondary contributions from C_α–C_β stretching, and ν_4 is a pyrrole ring breathing mode[16] and so might also be weakly affected by a change in a_{1u} orbital energy.

Effects on the $e_g(\pi^*)$ Orbital. The spectral data plotted as it is in Figure 1 essentially eliminates the parameter A_{1g}' from consideration, but it must also vary to account for the observed spectra. To see this note that both parts of eq 5 when added give

$$A_{1g}' = \tfrac{1}{2}(E_B + E_Q) \qquad (10)$$

That is, A_{1g}' is equal to the average of the energies of the Q and B transitions independent of the other parameters. Figure 5 shows a plot of experimental values of $^1/_2(E_B + E_Q)$ vs. the calculated values of A_{1g} from the analysis of the data in Figure 1. From eq 1 and 2 we can calculate an expression for the slope of such a plot. It is

$$\frac{\Delta A_{1g}'}{\Delta A_{1g}} = \frac{\tfrac{1}{2}(2\delta_e - \delta_{a_1} - \delta_{a_2})}{\tfrac{1}{2}(\delta_{a_1} - \delta_{a_2})} \qquad (11)$$

(14) Shelnutt, J. A. *J. Am. Chem. Soc.* **1983**, *105*, 774–778.
(15) Shelnutt, J. A.; Ondrias, M. R. *Inorg. Chem.* **1984**, *23*, 1175.
(16) Abe, M.; Kitagawa, T.; Kyogoku, Y. *J. Chem. Phys.* **1978**, *69*, 4526–4534.

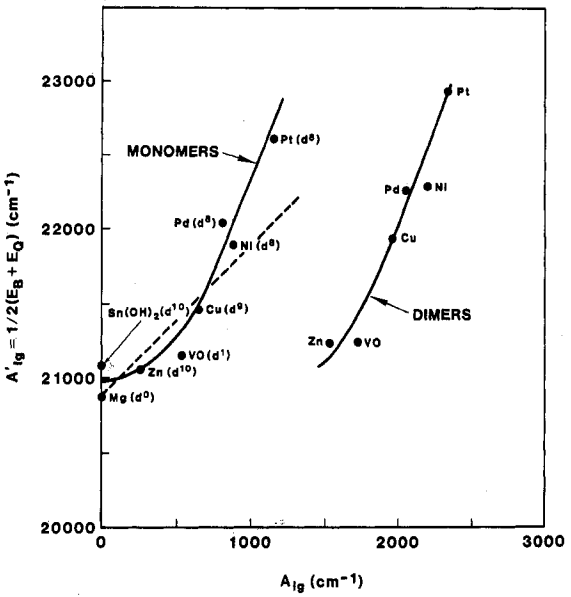

Figure 5. Plot of experimental values of $^1/_2(E_B + E_Q)$ vs. the values of A_{1g} obtained from fitting the data in Figure 1.

where δ_e, δ_{a_1}, and δ_{a_2} are changes in energy of the e_g, a_{1u}, and a_{2u} orbitals, respectively.

For metal-substitution effects we have assumed $\delta_{a_1} = 0$, therefore

$$\frac{\Delta A_{1g}'}{\Delta A_{1g}} = 1 - 2\frac{\delta_e}{\delta_{a_2}} \tag{12}$$

If δ_e also vanishes then we should obtain a linear plot with slope 1. For the metals for which A_{1g} is less than about 800 cm^{-1} the slope is close to 1, but for the metals with values of A_{1g} larger than 800 cm^{-1} the slope is closer to 2–3. Thus, δ_e is apparently small for all metals except platinum and palladium. For these two metals, however, δ_e is positive and about equal to $-\delta_{a_2}$ ($\delta_{a_2} < 0$). The shifts in $e_g(\pi^*)$ energy for Pd and Pt are illustrated in Figure 4. These metals belong to the second and third row transition series and have enhanced back-bonding capabilities. Filled d_π metal orbitals may interact more strongly with the antibonding $e_g(\pi^*)$ orbitals and raise the e_g energy. It has previously been noted that metals from different periods of the periodic table show distinct correlations between the frequencies of the core-size marker lines and E_Q.[15] Since $E_Q = A_{1g}' - A_{1g}''/\cos 2\theta$, A_{1g}' might be different for each row of the periodic table with the correlation for metals in a row given by differences in θ and, proportionately, A_{1g}.

We have speculated that it is the a_{1u} that moves up by about 2500 cm^{-1} upon dimerization and $\delta_{a_2} = 0$. Therefore, the change in A_{1g}' upon dimerization is

$$\Delta A_{1g}' = \tfrac{1}{2}(2\delta_e - \delta_{a_1}) \tag{13}$$

or

$$\delta_e = \Delta A_{1g}' + \tfrac{1}{2}\delta_{a_1} \tag{14}$$

Comparing monomers and dimers with the same metal in Figure 5 shows that A_{1g}' increases by about 300 ± 200 cm^{-1} upon dimerization. Therefore, e_g increases by about 300 + $^1/_2$(2500) = 1550 cm^{-1} upon dimerization regardless of the metal. This dimer shift in $e_g(\pi^*)$ is illustrated in Figure 4.

The charge density distribution of the $e_g(\pi^*)$ orbital has similarities with both the a_{1u} and a_{2u} orbitals with charge density at all atoms of the ring. It is, therefore, not surprising that the e_g-orbital energy changes for interactions with the ring that exclusively affect either the a_{1u} orbital (dimerization) or the a_{2u} orbital (metal variation).

Effect of Dimerization on Intrinsic Electronic Transition Dipoles. Dimerization also affects the transition dipole of the 50/50 mixed states. The ratio of the dipoles of the 50/50 mixed configurations r/R changes from −0.173 to 0.022 upon dimerization. In terms of the transition dipoles for the configurations, R_1 and R_2, $r/R = (R_2 - R_1)/(R_1 + R_2)$. Calculations give $R_1 \approx R_2 \approx 2$ Å, in agreement with a nearly vanishing r/R ratio. Based on calculated transition moments for the porphyrin without a metal present, r/R is estimated in the range from 0.024 to 0.033[7] in good agreement with the dimer value, but far from the monomer ratio. Recent MO calculations for copper porphine give an estimate of −0.030 for r/R, closer to the monomer value.[17]

Changes in R_1 result from changes in the molecular orbital coefficients of a_{1u} and e_g; R_2 depends on the a_{2u} and e_g orbital coefficients. Since it is primarily a_{1u} that changes energy upon dimerization, we can speculate that R_1 increases by almost 0.2 Å.

Apparently the changes in orbital coefficients that result from putting different metals in the core do not significantly change R_2 relative to R_1, or else a single value of r/R would not produce a curve that would fit the data in Figure 1. Hence, it may be somewhat fortuitous that the family of curves like those generated in Figure 2 can fit the data, i.e., that only the parameter A_{1g} is a function of the metal.

Conclusions

The four-orbital model in its general form ($r/R \neq 0$ and $\theta \neq 0$) has the richness of structure to quantitatively predict various trends in experimental spectral data for metallouroporphyrin monomers and dimers. A relationship between the splitting of the α and Soret bands and the ratio of their dipole strengths is theoretically predicted when only the separation of the a_{1u} and a_{2u} orbitals is varied and other parameters of the model are held constant. This relationship is observed when the metal in the porphyrin ring is varied systematically. Fitting this data (Figure 1) we arrive at values for two of the orbital parameters—the two-electron CI matrix element and the ratio of transition dipoles for the 50/50 mixed configurations.

A considerably different dependence of $E_B - E_Q$ on q_Q^2/q_B^2 is observed for the dimers. Nevertheless, a second value for the ratio of intrinsic transition dipoles provides a fit for the dimer data also. An analogous treatment in which exciton coupling is included, in addition to the "solvent" effect considered in this work, indicates that the solvent effect is at least comparable to the exciton coupling.[10] In the range of parameters necessary to fit the dimer spectral data the dipole–dipole exciton coupling causes a shift of theoretical curves shown in Figure 2 along the $E_B - E_Q$ axis much like a change in A_{1g}'' does. The large scatter in the data in Figure 1 does not allow a quantitative determination of the relative contributions from "solvent" and exciton coupling effects.

A further analysis of the spectral data, using other aspects of the orbital properties and the interactions involved, suggest that the metal–porphyrin interaction primarily influences the $a_{2u}(\pi)$ orbital energy with some effect of back-bonding on $e_g(\pi^*)$ for metals of the second and third row transition metals. The solvent effect of dimerization apparently affects mainly the $a_{1u}(\pi)$ orbital with a secondary shift in the $e_g(\pi^*)$ orbital energy. Shifts in the Raman marker lines are essential in distinguishing which orbitals (a_{1u} or a_{2u}) are influenced by the metal–porphyrin and porphyrin–porphyrin interactions.

Acknowledgment. This work was performed at Sandia National Laboratories and supported by the United States Department of Energy Contract DE-AC04-76-DP00789 and the Gas Research Institute Contract 5082-260-0767.

Registry No. VO(MV^{2+})U (U = uroporphyrin), 86472-10-8; Mg(Pyr)U (U = uroporphyrin), 92011-52-4; $Sn(OH)_2$U (U = uroporphyrin), 92011-53-5; platinum uroporphyrin, 91798-65-1; nickel uroporphyrin, 84098-84-0; copper uroporphyrin, 78991-92-1; zinc uroporphyrin, 55972-25-3; palladium uroporphyrin, 91841-54-2.

(17) Shelnutt, J. A.; Straub, K. D.; Rentzepis, P. M.; Gouterman, M.; Davidson, E. R. *Biochemistry*, in press.